Chapter

Lead-Free Perovskite Nanocomposites: An Aspect for Environmental Application

Manojit De

Abstract

Perovskites possess an interesting crystal structure and its structural properties allow us to achieve various applications. Beside its ferroelectric, piezoelectric, magnetic, multiferroic, etc., properties, these branches of materials are also useful to develop materials for various environmental applications. As the population is increasing nowadays, different type of environmental pollution is one of the growing worries for society. The effort of researchers and scientists focuses on developing new materials to get rid of these individual issues. With modern advances in synthesis methods, including the preparation of perovskite nanocomposites, there is a growing interest in perovskite-type materials for environmental application. Basically, this chapter concludes with a few of the major issues in the recent environment: green energy (solar cell), fuel cell, sensors (gas and for biomedical), and remediation of heavy metals from industrial wastewater.

Keywords: perovskite, nanocomposite, fuel cell, sensors, solar cell, heavy metals, wastewater treatment

1. Introduction

Perovskites possess a very interesting crystal structure; are basically a combination of three basic crystal structures (simple cubic structure, body center cubic structure, and face-centered cubic structure). The extraordinary range of structure and properties interplay of perovskites makes them an exceptional research field for different branches like materials science, physics and solid-state chemistry. A wide range of unique functional materials and device ideas can be predicted through a basic understanding of the correlation between structural and chemical compatibility.

The perovskite structure is shown to be the single most adaptable ceramic host. Inorganic perovskite-type oxides are attractive compounds for varied applications due to its large number of compounds, they exhibit both physical and biochemical characteristics and their nano-formulation have been utilized as catalysts in many reactions due to their sensitivity, unique long-term stability, and anti-interference ability. Some perovskite materials are very hopeful applicants for the improvement of effective anodic catalysts performance. Depending on perovskite-phase metal oxides' distinct variety of properties they became useful for various applications they are newly used in electrochemical sensing of alcohols, glucose, hydrogen-peroxide, gases, and neurotransmitters. Perovskite organometallic halide showed efficient essential properties for photovoltaic solar cells.

1.1 The basic structure of perovskites

Figure 1 depicts the ideal perovskite structure. In the ideal crystal structure of perovskite with general formula ABX_3; where "A" and "B" are generally metal cations and "X" is an oxide or halide like Cl, Br, I, etc., "A" can be Ca, K, Na, Pb, Sr, and other rare-earth metals which occupy the 12-fold coordinated sites between the octahedra. "X" forms the BX_6 octahedra where B located at the center of octahedra. Perovskite can be described as consisting of corner-sharing [BX_6] octahedra with the A-cation occupying the 12-fold coordination site formed in the middle of the cube of eight such octahedra. In an ideal cubic unit cell of perovskite, Wyckoff positions for A- ion is at cube-corner positions (0, 0, 0); ion B sites at body center position (1/2, 1/2, 1/2) and ion X sits at face-centered positions (1/2, 1/2, 0). **Figure 2** shows the elements which can be in A-site, B-site from the periodic table.

In ideal perovskite such as $SrTiO_3$ [3], $CsSnBr_3$ [4], etc., there is no such distortion in the unit cell. There are many different types of lattice distortions that can happen due to the flexibility of bond angles within the ideal perovskite structure [5].

i. Distortion in BX_6 octahedra, by the Jahn-Teller effect.

ii. Off-center displacement of B-cation in BX_6 octahedra, this one of the causes for ferroelectricity in these type of materials.

iii. So-called tilting in octahedra framework, usually occurring as a result of too small A-cations at cuboctahedral site.

iv. Ordering of more than one type of cations A or B, or of vacancies.

v. Ordering of more than one kind of anions X, or of vacancies.

The different physical properties (mainly electronic, magnetic, dielectric, and piezoelectric properties) of perovskite materials are crucially dependent on these distortions. The distortion as a consequence of cationic substitution can be used to fine-tune physical properties exhibited by perovskite.

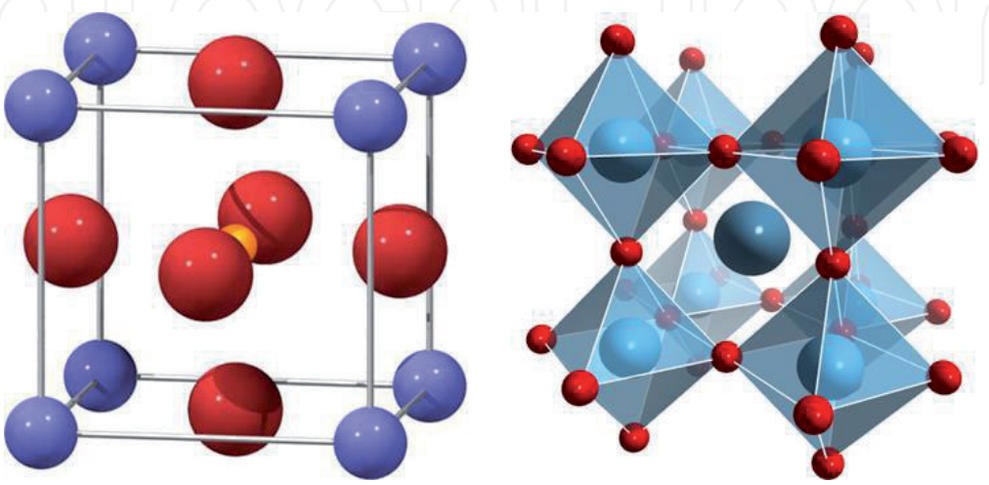

Figure 1.
The ideal structure for perovskite; blue balls represent the A-site, yellow ball shows the B-site, and magenta balls showing the position of X anion (face center position) [1].

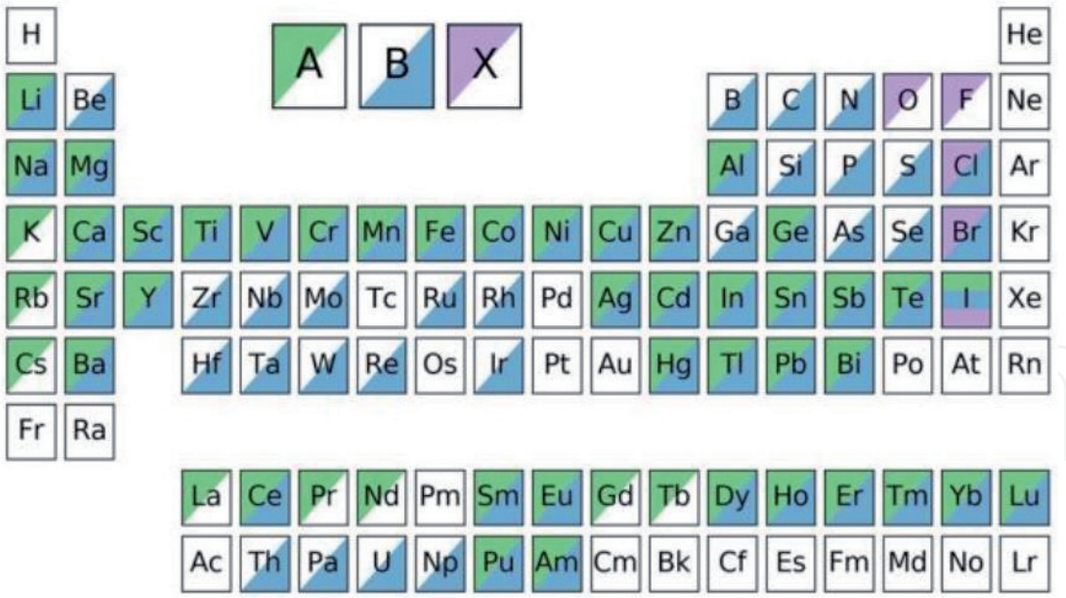

Figure 2.
A map of the elements in the periodic table which can occupy the A, B, and/or X sites [2].

In the case of perovskite structure (closed packed), A-cation must fit among four BX_6 octahedra. Each A-cation is surrounded by 12 nearest X-anions (12-fold coordination). Therefore A-cations have limited space to accommodate itself in the interstitial position. In the case of ideal perovskite structure, the cell axis (a) is geometrically related to the ionic radii (r_A, r_B, and r_X) as described in the following equation.

$$a = \sqrt{2}\left(r_A + r_X\right) = 2\left(r_B + r_X\right) \tag{1}$$

The ratio of the two expressions for the cell length is called Goldschmidt's tolerance factor (t) and it allows us for evaluating the degree of distortion in the unit cell. The expression for Goldschmidt's tolerance factor [6] is as follows.

$$t = \frac{\left(r_A + r_X\right)}{\sqrt{2}\left(r_B + r_X\right)} \tag{2}$$

where r_A is the radius of A-cation is, r_B is the radius for B-cation and r_X is the radius for X-anion.

1.2 Why lead-free?

Lead (and its oxide form) is highly hazardous and its harmfulness is further improved due to its volatilization at high temperature mainly during calcination and sintering causing environmental pollution during different sample preparation techniques [7]. According to the European Union (EU), hazardous substances like lead and other heavy metals is planning to strictly prohibit [8, 9].

1.2.1 Toxicity effects of lead

The main indications of lead poisoning are tiredness, muscles and joints pain, abdominal uneasiness, etc. Sometimes the deposition of lead sulfide

can be found out in the dental margin of the gums of the patients having poor dental hygiene. Lead harming has been considered as a health hazard, for its bad effects on neurological and cerebral development [10–12]. The main route of absorption in adults is the respiratory region where 30–70% of inhaled lead (typically the inorganic form like oxides and salts) goes into the cardiovascular system. The maximum tolerance of lead in blood ranges from 1.45 to 2.4 mol L^{-1} (30–50 g 100 mL^{-1}) with a provision of 6 monthly observations [13]. Basically, lead has few significant biochemical properties that give toxic effects on the human biological system. (i) As lead is electropositive in nature, it shows a very high affinity for the enzymes, which are necessary for the synthesis of hemoglobin. (ii) The divalent lead behaves similarly to calcium preventing mitochondrial oxidative phosphorylation as a result intelligence quotient (IQ) got reducing. (iii) The transcription of DNA can also disturb by lead by interacting with binding protein and nucleic acids [14, 15]. **Figure 3** illustrated the adverse effect of lead on the human body.

Bearing in mind the hazardous effect of Pb in Pb-based compounds, the research communities focused on designing the materials which are basically Pb-free. Hence, this chapter concludes with some Pb-free perovskite-type materials for the environmental application point of view.

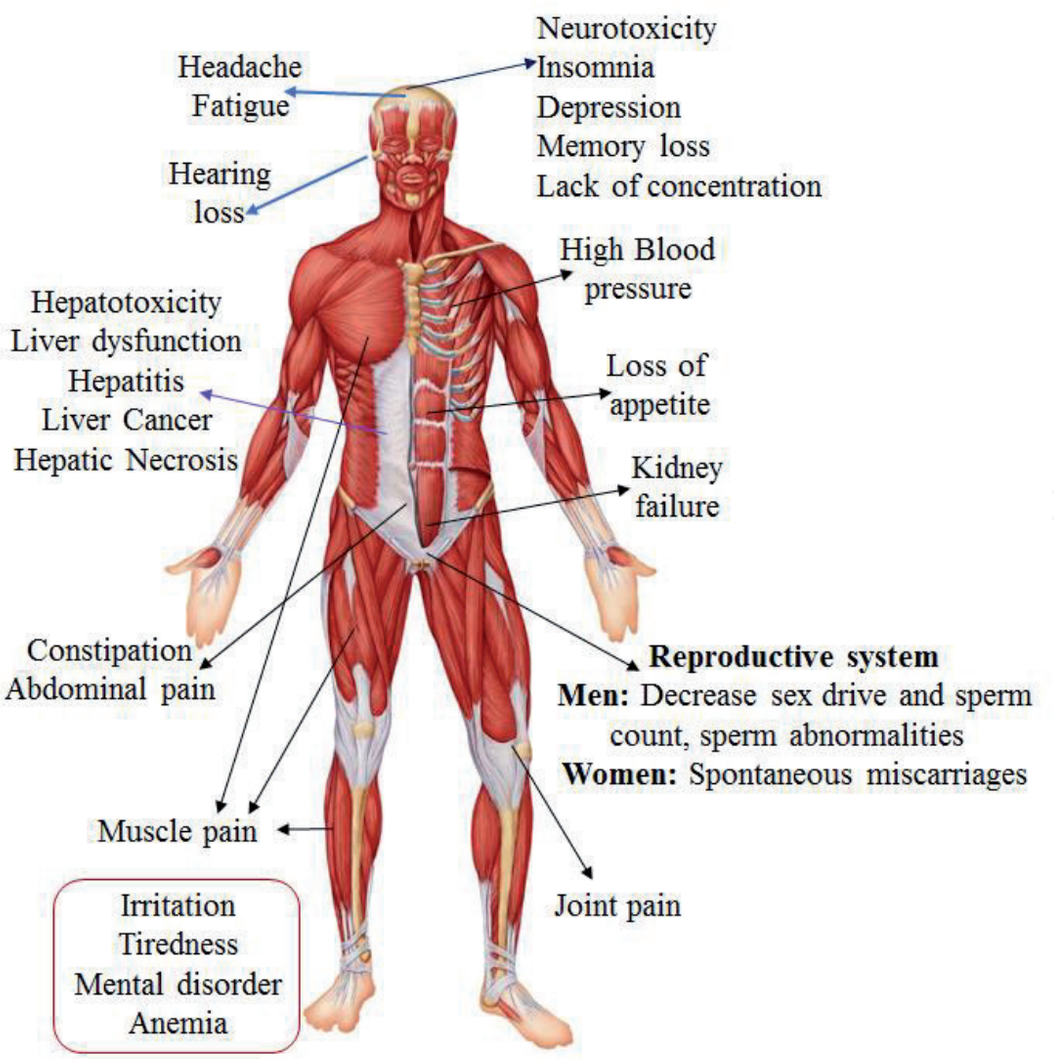

Figure 3.
Schematic diagram for toxic effect of lead on human body.

2. Application of Pb-free perovskites from a different aspect of environmental

2.1 Perovskites as solid oxide fuel cells

Recently, the inorganic perovskite-type of oxide nanomaterials have been widely applied in the processing of chemically modified electrodes [16, 17]. They have acknowledged considerable attention in the last few decades because of their catalytic activity in diverse processes like purification of waste gas and catalytic combustion.

In the fuel cell, there is a direct conversion of chemical energy into electrical energy similar to a battery. These are attractive because of their great efficiency, low emission, almost zero pollution (basically noise pollution). The solid oxide fuel cells (SOFCs) have come into the picture as effective substitutions to the combustion engines due to their prospective to minimize the environmental impact of the use of conventional fossil fuels. Perovskite oxides exhibited attractive properties like a high electrical and ionic conductivity similar to that of metals and the perfect mix of these two types [18]. This mixed conduction properties of perovskite oxides are advantageous for electrochemical reaction. The working principle of a SOFC is depicted by **Figure 4** [19]. The perovskite $Ba_{0.5}Sr_{0.5}Co_{0.8}Fe_{0.2}O_{3-\delta}$ used as an effective cathode for intermediary SOFC reported by Shao and Haile. This cathode unveiled the maximum power density of 402 and 1010 mW cm^{-2} at 500 and 600°C, respectively [20]. The combination of single and double perovskite oxide $Ba_{0.5}Sr_{0.5}(Co_{0.7}Fe_{0.3})_{0.6875}W_{0.3125}O_{3-\delta}$ (B-SCFW) was investigated by Shin et al. [21] for self-assembled perovskite composites for SOFC. In contrast, Goodenough reported that the double perovskite $Sr_2MgMnMoO_{6-\delta}$ can act as an anode material for SOFC with dry methane as the fuel and it shows maximum power density of 438 mW cm^{-2} at 800°C. This anode material exhibited long-term stability and having oxygen insufficiency, as well as some good environmental effects like tolerance to sulfur, stability in reducing atmosphere [22]. **Table 1** enlisted with some perovskites used as anode and cathode for SOFCs.

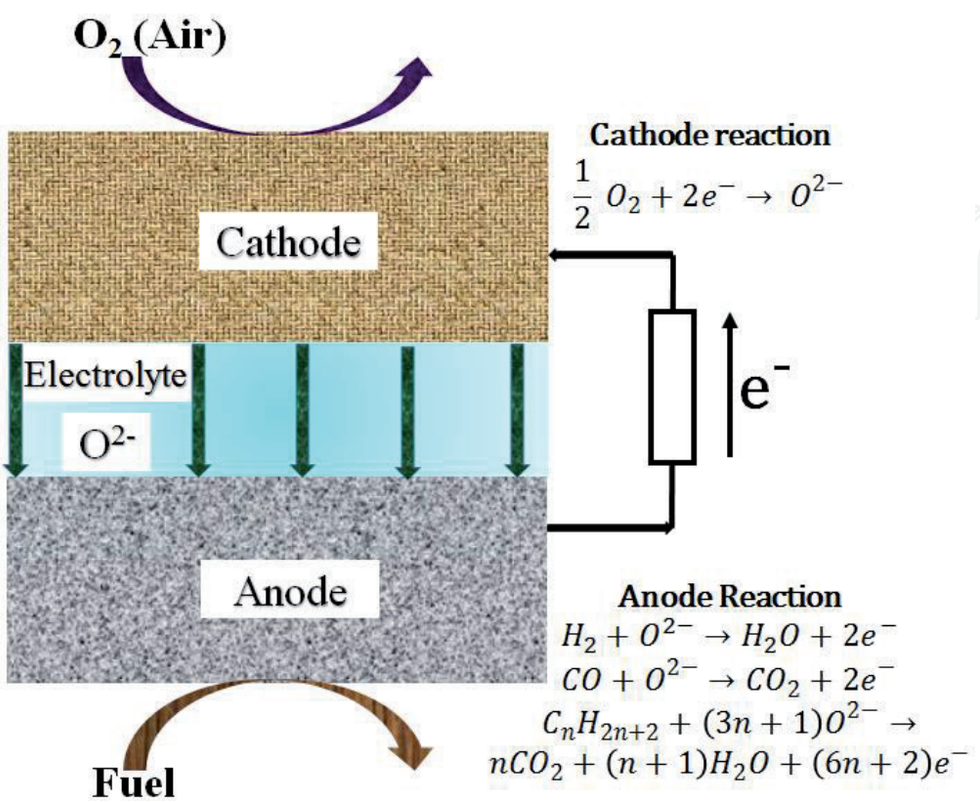

Figure 4.
Diagram illustrates the working principle of SOFC [19].

Perovskite compositions	Anode/ cathode In cell	Fuel used	Operating temperature (°C)	Maximum power density ($mW\ cm^{-2}$)	Reference
$Ba_{0.5}Sr_{0.5}Co_{0.8}Fe_{0.2}O_{3-\delta}$	Cathode	Humidified H_2 (~3% H_2O)	500	402	[20]
			600	1010	
$Ba_{0.5}Sr_{0.5}Co_{0.2}Fe_{0.8}O_{3-\delta}$	Cathode	Humidified H_2	800	266	[23]
$NdFeO_3$	Anode	Sulfur vapor or SO_2	620	0.154	[24]
			650	0.265	
$La_{0.6}Sr_{0.4}Fe_{0.8}Co_{0.2}O_3$	Cathode	Glycerol	800	Not reported	[25]
$Sm_{0.5}Sr_{0.5}CoO_{3-\delta}$	Cathode	Not reported	700	936	[26]
$La_{0.8}Sr_{0.2}Cr_{0.97}V_{0.03}O_3$	Anode	Dry methane	800	Not reported	[27]
$La_{0.75}Sr_{0.25}Cr_{0.5}Mn_{0.5}O_3$	Anode	Methane	Not reported	Not reported	[28]

Table 1.
Summary report of few Pb-free perovskites used in SOFCs.

2.2 Perovskites as sensor

2.2.1 Perovskites as glucose sensor

It is very essential to determine hydrogen peroxide (H_2O_2) and glucose analytically in any aspect of our daily life. In environmental waste management, chemical and food industries, and medical diagnostics H_2O_2 widely used as one of the most important oxidizing agents [29]. On the other hand, glucose represents a fundamental component in human blood that delivers energy through the metabolic process. If in human blood, the glucose concentration fluctuates than the normal range of 80–120 mg dL^{-1} (4.4–6.6 mM) is related to the metabolic disorder from insulin insufficiency and hyperglycemia, the so-called diabetes mellitus [30]. To perform the diagnosis and supervision of such health issue it is necessary a tight observation of glucose level of blood. Hence, it is very significant to make the biosensors for the sensitive determination of glucose and H_2O_2. Basically, there are two types of glucose sensors available: enzymatic and non-enzymatic. Different types of enzymatic glucose sensors were constructed and used in the literature exhibiting the advantages of simplicity and sensitivity. However, enzymatic glucose sensors suffered from the lack of stability and the difficult procedures required for the effective immobilization of the enzyme on the electrode surface. The lack of enzyme stability was attributed to its intrinsic nature because the enzyme activity was highly affected by poisonous chemicals, pH, temperature, humidity, etc. As a result, most attention was given for a sensitive, simple, stable, and selective non-enzymatic glucose sensor. Different novel materials were proposed for the electrocatalytic oxidation of glucose like noble nanometals, nanoalloys, metal oxides, and inorganic perovskite oxides. Inorganic perovskite oxides as nanomaterials exhibited fascinating properties for glucose sensing like ferroelectricity, superconductivity, charge ordering, high thermopower, good biocompatibility, catalytic.

Wang et al. utilized a carbon paste electrode (CPE) modified with $LaNi_{0.5}Ti_{0.5}O_3$ (LNT) as a promising nonenzymatic glucose sensor. This glucose sensor displayed a perfect electrochemical activity and was used to quantify of glucose with great sensitivity of 1630.57 μA mM^{-1} cm^{-2} and a low detection limit of 0.07 μM. This glucose sensor also demonstrated an excellent reproducibility, long-term immovability, as well as outstanding selectivity with no interference from the common interfering

substances such as dopamine, ascorbic acid, and uric acid [31]. The perovskite-spinel type composite oxide $LaNi_{0.5}Ti_{0.5}O_3$-$NiFe_2O_4$ with different compositions was demonstrated as the glucose sensor by Wang et al. This material also exhibits admirable reproducibility, stability and selectivity in glucose sensitivity with a linear signal-to-glucose concentration range of 0.5–10 mM and a detection limit (S/N = 3) of 0.04 mM [32]. Furthermore, $La_xSr_{1-x}Co_yFe_{1-y}O_{3-\delta}$ (x = 0.6; y = 0.0 and 0.2) perovskites were studied as electro-catalytic materials for H_2O_2 and glucose electrochemical sensors by Liotta et al. [33]. The group of Atta et al. has reformed $SrPdO_3$ perovskite with gold nanoparticles to be employed as a non-enzymatic voltammetric glucose sensor. This nanocomposite disclosed an excellent performance to glucose sensing in terms of highly reproducible response, high sensitivity, low detection limit, appreciable selectivity, long-standing stability [34]. He et al. depicted that the perovskite oxide $La_{0.6}Sr_{0.4}CoO_{3-\delta}$ can provide superior electro-oxidation activities (to H_2O_2 and glucose) over $La_{0.6}Sr_{0.4}Co_{0.2}Fe_{0.8}O_{3-\delta}$ and $LaNi_{0.6}Co_{0.4}O_3$ that translates to good H_2O_2 or glucose detection performance. They have modified the sensor by making composite with reduced graphene oxide (RGO) and $La_{0.6}Sr_{0.4}CoO_{3-\delta}$ for exhibiting higher detection properties and improved selectivity [35].

2.2.2 Perovskites as a gas sensor

The clean air is undoubtedly most necessary than water for human health, but unfortunately, human activities accompanying socioeconomic developments are the vital pollution sources. So, it is very important to closely observe the quality of the air, including the indoor air quality (IAQ) as we spent most of our time (~90%) of our time in the indoor climate, to prevent different unusual symptoms [35–37]. Thus, researchers and scientists across the whole globe have been developing new and advanced material based innovative methods for consistent and careful detection of gases and volatile organic compounds (VOCs) hazardous to human and environmental health [38, 39]. The environmental worries about health hazards due to the existence of poisonous gases, for example, CO, CO_2, NO_2, O_3, etc., and subsequent safety regulations have demanded the enhanced use of sensors in various sceneries from the industrial sites to automobiles, the different workplaces and even homes. Among the several toxic gases, CO and NO_2 are the most harmful air pollutants and are dangerous for animals, plants and as well as human beings. The Occupational Safety and Health Administration (OSHA) have also announced the limit lowest tolerance for these type of gases in a particular time period, for example, the limits for CO and NO_2 gases are ~20 ppm and ~5 ppm over the period of 8 h respectively. Over-acquaintance to these gases could be the reason for diseases and in dangerous cases even loss of human life [40]. There are a number of features that the materials can have to be utilized as gas sensors, explicitly, an excellent similitude with the target gases, easy to synthesize, thermal stability, appropriate electronic structure, and adaptation with present technologies. The perovskite oxides are interesting materials as gas sensors because of their ideal bandgap, excellent thermal stability and the size difference between the A- and B-sites cations, tolerating different dopants addition for monitoring the catalytic properties and their semiconducting properties. Lots of perovskites were synthesized to utilize as gas sensors for detecting different hazardous gases. **Table 2** enlisted with different perovskite oxides for various gas sensing applications.

2.3 Perovskites as solar cell materials

The consumption of energy has been continuously increasing globally and limitations of sources of fossil fuels leading to perform the research on sustainable, environment-friendly, and renewable energy sources. Due to the abundance of sun rays on

Perovskites	Sensing for	Response ratio %	Reference
$LaCoO_3$	CO	Under 5000 ppm CO at 500°C, the thick film sensor achieved a high sensing response of ~279.86	[41]
$La_{0.9}Ce_{0.1}CoO_3$	CO	240% with respect to 100 ppm CO in air	[42]
Ca modified $LaFeO_3$	SO_2	Maximum resistive response of 3 ppm SO_2 was detected at ~275°C by the $LaCaFeO_3$ samples, and it shows 15% higher efficiency than $LaFeO_3$	[43]
$NdFe_{1-x}Co_xO_3$	CO	1215% at 170°C for 0.03% CO gas	[44]
$LaFeO_3$	Ethanol	Not reported	[45]
Ag-$LaFeO_3$	Methanol	The maximum response to the other test gases is 8	[46]
Ag-$LaFeO_3$	Formaldehyde	Best response to 0.5 ppm formaldehyde (24.5) at 40°C	[47]
$SrFeO_3$	Ethanol	Not reported	[48]
$LaFeO_3$	NO_2	Not reported	[49]
$GaFeO_3$	Ethanol	Ethanol sensing down to 1 ppm at 350°C	[50]
$SrTi_{1-x}Fe_xO_{3-\delta}$	Hydrocarbons	Not reported	[51]
α-Fe_2O_3/$LaFeO_3$	Acetone	Response 48.3% at 100 ppm concentration at 350°C	[52]
$YCo_{1-x}Pd_xO_3$	CO, NO_2	Different for the different composition	[53]
$ZnSnO_3$	n-Propanol gas	The detection limit of $ZnSnO_3$ nanospheres to 500 ppb n-propanol gas could reach 1.7	[54]
$LaFeO_3$ and rGO-$LaFeO_3$	NO_2 and CO	Response 183.4% for 3 ppm concentration of NO_2 at a 250°C	[55]
$BaTiO_3$/$LaFeO_3$ nanocomposite	Ethanol	Response 102.7% to 100 ppm ethanol at 128°C	[56]
Ba-$BiFeO_3$	Ethanol	Temperature dependent sensing performance toward 100 ppm ethanol gas; maximum sensitivity at 400°C	[57]
La doped $BiFeO_3$	Acetone	The morphotropic phase boundary (MPB) phase $Bi_{0.9}La_{0.1}FeO_3$ shows ultra-low concentration detection of 50 ppb acetone	[58]
Pr doped $BiFeO_3$	Formaldehyde	50 ppm, 190°C, R_{gas}/R_{air} = 17.6	[59]
$BaTiO_3$ thick films	H_2S	$BaTiO_3$ sensor operated at 350°C	[60]
Sr doped $BaTiO_3$	NH_3 and NO_2	0.2 mol% doping of Sr showed enhanced performance for sensing of both NO_2 and NH_3 gases at room temperature	[61]
$BaSnO_3$	SO_2	10 ppm of SO_2	[62]
$BaSnO_3$	LPG	Addition of noble metal Pt, the operating temperature decreases and the sensitivity improved but also imparted partial selectivity for the detection of LPG	[63]
$LaBO_3$ (B = Fe, Co)	Acetone	At a low operating temperature of 120°C showed that the $LaFeO_3$ NFs based sensor displayed high stable and selective response toward 40 ppm acetone with fast response and recovery time of 14 and 49 s	[64]

Table 2.
Tabulated with different perovskite oxides for various gas sensing applications.

our globe, the transformation of sunlight into electricity is one of the most favorable studies for increasing energy demands without having any adverse effect on the global climate. Solar cell technology offers an eco-friendly and renewable energy path to convert photon energy into electricity openly [65]. Nowadays a large effort has been put in the research to develop high efficiency, low-cost photovoltaic devices but regrettably did not succeed yet. During the last decade, research into perovskite solar cells (PSCs) has increased and it also been nominated as a runner-up for the top 10 breakthroughs research of 2013 by the editors of Science [66]. The organic-inorganic perovskite having the general formula ABX_3 where A is cesium (Cs), methylammonium (MA), or formamidinium (FA); B is Pb or Sn; and X is Cl, Br, or I, have recently appeared as an exciting class of semiconductors which can act as solar cell materials [67]. These organic-inorganic halide perovskite solar cells have shown substantial improvement of power conversion efficiency (PCE) from the preliminary efficiency of 3.8% [68] to about 22.1% [69]. The maximum theoretical power conversion efficiency accomplished by perovskite ($CH_3NH_3PbI_3$) is about 31.4% [70]. The organic-halide perovskites owing extraordinary performance because of some unique properties like (i) high absorbing coefficient, (ii) high charge carrier mobility, (iii) long diffusion length, (iv) direct bandgap which can be engineered easily and (v) moreover easy to fabricate [71]. The normally used Pb-based perovskites have numerous advantages such as (i) large diffusion length, (ii) absorption range, (iii) low exciton binding energy, and (iv) high carrier mobility. Conversely, the Pb-based perovskite solar cell has a serious toxic issue on both humans and the environment [72]. Generally, PV panels are positioned on the roof of houses or in the open field, their exposure to rainfall is inescapable. In the manifestation of rain and moisture the degradation of PbI_2 may cause mild to acute health issues, like effects on cardiovascular, neurological, reproductive system [73] mainly it is carcinogenic [72, 74] Additionally, lead pollution has severe effects on water and soil resources and emission of greenhouse gasses [75, 76]. Hence, in PSCs, it is essential to replace Pb for economical green energy conversion devices which may use mankind in future endeavors [77].

To develop Pb-free PSCs, Sn^{2+} metal cation was the first another candidate to replace Pb^{2+} as of its comparable electronic configuration and effective ionic radius (Sn^{2+}: 115 pm) to lead (Pb^{2+}: 119 pm) [78]. The hybrid organic-inorganic halide perovskites having the chemical formula of $AM^{IV}X^{VII}_3$, where A represents a small monovalent organic molecule, M^{IV} is a divalent group-IVA cation and X^{VII} is a halogen anion, have recently attracted remarkable attention in the photovoltaic community $MASnI_3$ and $MASn\text{-}(I_{3-x}Br_x)$ have been shown to the efficiencies of 6.4% [79] and 5.73% [80] respectively. $CH_3NH_3SnI_3$, $HC(NH_2)_2SnI_3$, $NH_2NH_3SnI_3$, and $NH_2(CH_2)_3SnI_3$ is the promising candidate to be a light sensitizer with suitable inorganic hole-transport material to achieve cost-effective and efficient lead-free perovskite solar cell [81, 82]. Gagandeep et al. uses the graphene as the layer for charge transport and is demonstrate the structure like n-Graphene/$CH_3NH_3SnI_3$/p-Graphene which shows the efficiency of 10.67–13.28% [83]. Giorgi et al. substituted Pb by TlBi ($MATl_{0.5}Bi_{0.5}I_3$) and InBi ($MAIn_{0.5}Bi_{0.5}I_3$) and depicted that these systems are quietly equivalent to $MAPbI_3$ and can be good replacements for PSCs [84]. Germanium is also assumed as a possible candidate for Pb substitution in halide perovskites. The theoretical structure and electronic properties of $AGeI_3$ (A = MA, FA, Cs) were investigated by Krishnamoorthy et al. [85]. There are several elements like: Bi [86–88], Sb [89–91], Ti [92], Cu [93, 94] that use to substitute Pb to decrease the lead pollution. The group of Song et al. has reported the photovoltaic application of Sn-based halide perovskite materials having the general formula $ASnI_3$ (A = Cs, methylammonium and formamidinium tin iodide as the representative light absorbers). Among all the perovskites, $CsSnI_3$ devices accomplished a maximum power conversion efficiency of 4.81% [95]. Nishimura et al. synthesized

GeI_2 doped $FA_{0.98}EDA_{0.01}SnI_3$ and GeI_2 doped $EA_{0.98}EDA_{0.01}SnI_3$ PSCs and shows the power conversion efficiency of 13.24% for lead-free perovskite solar cell has been demonstrated with mixed cation and surface passivation [96].

2.4 Removal of heavy metals from wastewater

To survive on this planet the clean air, water, and foods are essential to all forms of life. The surface and the groundwaters are only the sources of clean water which help to all living systems as well as human activities such as consuming, irrigation of crops, industrial application, etc. [97]. Water pollution is one of the most world-wide common issues as the population outbursts and industrial evolutions are there. Day by day, the heavy metals (maybe in the form of ions) are released into water bodies by various industries [98] and are exceedingly water-soluble, non-decomposable, oncogenic agents and cause adverse health complications on the animals as well as human beings. Wastewaters coming out from various industries contain many heavy metal ions, for example, Cu^{2+}, As^{5+}, Ni^{2+}, Sb^{5+}, Zn^{2+}, Cd^{2+}, and Pb^{2+} [99]. In addition to heavy metal ions, the different organic and inorganic dyes are alternative pollutant releases from different industries for example papers, textiles, and plastics where the dyes are used for coloring their product and also generate significant volumes of wastewater. Many of these dyes containing heavy metal ions have a tendency to store in the living entities causing a different type of diseases and disorders [100–102]. Hence, it is essential to purify the metal-contaminated water before its discharge to the environment. Among all compare to current methods to remove heavy metal from the contaminated water [100, 101] adsorption method is the most likely one because it low cost-effective, high efficiency, and simple to run.

2.4.1 Heavy metals from contaminated water

The group of Zhang et al. synthesized the porous nano-calcium titanate microspheres via a citric acid assisted modified sol-gel method and used for absorption of heavy metals like lead, cadmium, and zinc [103]. Haron et al. reported that the nano-crystalline $LaGdO_3$ perovskite was synthesized by the co-precipitation method could adsorb heavy metal ions (Cd^{2+} and Pb^{2+}) which should be the attention in an application such as wastewater treatment [104]. Zhang et al. synthesized porous nano-barium-strontium titanate via sol-gel method using sorghum straw as a template and investigate about adsorption mechanism of Pb, Zn, and Cd from contaminated water [105]. $LaFeO_3$ nanoparticles were synthesized by Rao et al. by the sol-gel method in presence of different chelating agents and these nanoparticles utilized for an adsorbent of the removal of heavy metal ions in particular cadmium ion. The $LaFeO_3$ sample prepared with succinic acid (SA) as a chelating agent shows a higher removal efficiency of Cd^{2+} ions from aqueous systems [106]. Zhang et al. investigated Sr modified $LaFeO_3$ and its structural and catalytic activity. $La_{0.8}Sr_{0.2}FeO_3$ contributed significantly enhanced activity in methane combustion and CO oxidation because the oxygen vacancies accelerated the dissociation of gaseous oxygen on the surface in CO oxidation and facilitated the diffusion of lattice oxygen from the bulk to the surface during CH_4 combustion [107]. The perovskite $LaAlO_3$ was manufactured using the co-precipitation method by Haron et al. The structural and efficiency of removal of heavy metal (Cd^{2+} and Pb^{2+}) were extremely investigated by them. The adsorption performance was studied which fit with the Langmuir isotherm. The results disclosed that $LaAlO_3$ perovskite showed high efficiency as heavy metal ions remover from the contaminated water. This adsorbent could be recycled with an EDTA solution and reprocessed with only slightly less efficient than that of the fresh sample [108]. The group of Chen et al. synthesized ternary photocatalyst $ZnTiO_3/Zn_2Ti_3O_8/ZnO$

heterojunction which displays excellent performance for the degradation of organic pollutants as well as reduction of heavy metal Cr(VI) ions from wastewater [109]. **Figure 5** schematically represent the heavy metal ion (Cd^{2+}) adsorb with $LaFeO_3$ perovskite prepared with the different chelating agent.

2.4.2 Heavy metals in wastewater from the textile industry

The growing population in our globe, demands to clothe and increase with the taming sense of fashion and lifestyle thus textiles are contrived to meet the growing demands. In several countries such as India and Sri Lanka; the production of textile becomes their source of income that subsidizes their gross domestic product (GDP). However, this has brought both significances to such countries either in a positive way which is an enhancement of the economy or in a negative way indorsed to environmental pollution. The textile industries have been adapted as the worst reprobates of pollution contributors [110]. Especially, in India, according to the Central Pollution Control Board [111], a total of 2324 textile industries are set up. The textile industries employ different types of dyes for the manufacturing of various fabric materials. In reality, about 1 million different dyes are found in the market [112] and roughly 700,000 tons of artificial dyes are produced per year [113]. The disposal of dyes in waters exemplifies a severe environmental issue due to the coinciding presence of various types of pollutants [114–116]. All traditional methods used for the treatment of dyes and/or heavy metals have limitations because of cost, efficiency and operational complications. Among all of them, adsorption was exposed as one of the most effective methods due to its simplicity in operation, adaptability, high-treatment efficiency and low cost, and hence it is extensively applied for wastewaters treatment [117–121].

The perovskite oxide $La_{0.9}Sr_{0.1}FeO_3$, capped with cetyl trimethyl ammonium bromide (CTAB) cationic surfactant, and used as a sorbent for the removal of the anionic Congo red (CR) dye from aqueous solutions was reported by Ali et al. [122]. The group of Chu et al. demonstrated the efficiency of Ag-$La_{0.8}Ca_{0.2}Fe_{0.94}O_{3-\delta}$ for the removal of organic and bacterial pollutants by catalytic peroxymonosulfate (PMS) activation. The oxygen vacancies in the B-site of perovskite enhances PMS activation and The SO_4• and •OH radicals enhance the biocidal activity [123]. Nanocrystalline $LaAlO_3$:Sm^{3+}:Bi^{3+} composites are used to adsorb Direct Blue-53 (DB-53) dye was reported by Pratibha et al. [124]. This adsorbent is good and promising in the adsorption capacity and is advantageous in the elimination of toxic and non-biodegradable pollutants from water. The group of Dong et al. hydrothermally synthesized perovskite $BaZrO_3$ in the form of hollow micro- and nano-sphere. This size-tunable $BaZrO_3$ hollow nanospheres exhibited an excellent adsorption performance for reactive dyes in acidic conditions and can be used as excellent circular adsorbents for removing reactive dyes. They show the adsorption capacities are over

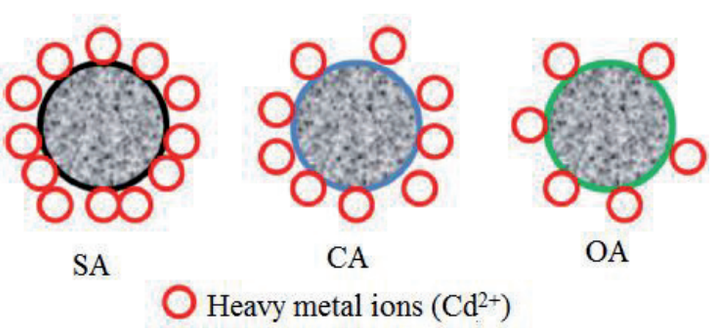

Figure 5.
Representation of the adsorption process over $LaFeO_3$ nanoparticles surfaces prepared using succinic acid (SA), citric acid (CA), and oxalic acid (OA) [106].

160 mg g^{-1} for different investigated dyes at a pH value of 2. The adsorbents were easily recovered by using a basic solution with the adsorption performance persistent and the desorption rate is more than 97 wt% [125]. Siddharth et al. synthesized the perovskite structure of Ti-doped $BaMnO_3$ ($BaMn_{0.85}Ti_{0.15}O_{2.93}$) and its enhanced photocatalytic degradation (~99%) as compared to $BaMnO_3$ toward toxic water impurities like RhB and MB dyes within 270 and 150 min under sunlight [126].

3. Conclusion

Nowadays, because of the increasing population and demand for natural resources is a global concern, hence, it is one of the origins of environmental pollution. Among all the pollutants, lead is one of the most hazardous materials. For the reason that the toxic effect of lead in lead-based materials, the researcher communities and scientists concentrated on synthesized lead-free materials possessing the same properties. Since the last two decades, the investigation on such materials enhances unexpectedly. Lead-free perovskite materials with excellent dielectric and piezoelectric properties belonging to the ferroelectric family and these reduce the adverse effect on the human body as well as the environment. Here this chapter concludes with different applications like SOFCs, sensors, solar cells, wastewater treatment of lead-free perovskite materials.

Thanks

I am whole heartily thankful to Dr. Sushrisangita Sahoo from Bhubaneshwar for continuous support during working in this chapter. I am thankful to Dr. S. Suganya from CSIR-Central Salt and Marine Chemicals Research Institute (CSMCRI), Bhavnagar, Gujrat, and Ms. Ananya Rout from NIT-Raipur, for their encouragement to start writing this chapter.

Author details

Manojit De[1,2]

1 Department of Pure and Applied Physics, Guru Ghasidas Vishwavidyalaya, Bilaspur, India

2 Department of Applied Physics, Chouksey Engineering College, Bilaspur, India

*Address all correspondence to: manojit.manojit.de1@gmail.com

References

[1] Levy MR. Crystal Structure and Defect Property Predictions in Ceramic Materials. London: Department of Materials, Imperial College of Science, Technology and Medicine. January 2005. Available from: https://spiral.imperial.ac.uk/bitstream/10044/1/11804/2/Levy-MR-2005-PhD-Thesis.pdf

[2] New Tolerance Factor to Predict the Stability of Perovskite Oxides and Halides. Available from: https://arxiv.org/ftp/arxiv/papers/1801/1801.07700.pdf

[3] Glazer AM. The classification of tilted octahedra in perovskites. Acta Crystallographica. Section B: Structural Crystallography & Crystal Chemistry. 1972;**28**:3384-3392

[4] Scaife DE, Weller PF, Fisher WG. Crystal preparation and properties of cesium tin(II) trihalides. Journal of Solid State Chemistry. 1974;**9**:308-314

[5] Aleksandrov KS. The sequences of structural phase transitions in perovskites. Ferroelectrics. 1976;**14**:801-805

[6] Goldschmidt VM. Die Gesetze der Krystallochemie. Die Naturwissenschaften. 1926;**21**:477-485

[7] Yugong W, Zhang H, Zhang Y, Jinyi M, Daohua X. Lead-free piezoelectric ceramics with composition of (0.97−x) $Na_{1/2}Bi_{1/2}TiO_3$-0.03$NaNbO_3$-x$BaTiO_3$. Journal of Materials Science. 2003;**38**:987

[8] United Nations Environment Programme. Nairobi; 2019. Available from: https://www.unenvironment.org/explore-topics/transport/what-we-do/partnership-clean-fuels-and-vehicles/lead-campaign

[9] Takenaka T, Nagata H. Current status and prospects of lead-free piezoelectric ceramics. Journal of the European Ceramic Society. 2005;**25**:2693-2700

[10] Gordon JN, Taylor A, Bennett PN. Lead poisoning: Case studies. British Journal of Clinical Pharmacology. 2002;**53**:451

[11] Barltrop D, Smith AM. Kinetics of lead interaction with human erythrocytes. Postgraduate Medical Journal. 1985;**51**:770

[12] Rabinowitz MB, Wetherill GW, Kopple JD. Kinetic analysis of lead metabolism in healthy humans. The Journal of Clinical Investigation. 1976;**58**:260

[13] Courtney D, Meekin SR. Changes in blood lead levels of solderers following the introduction of the control of lead at work regulations. Occupational Medicine. 1985;**35**:128

[14] Goering PL. Lead-protein interactions as a basis for lead toxicity. Neurotoxicology. 1993;**14**:45

[15] Chisolm JJ Jr. Treatment of lead poisoning. Modern Treatment. 1971;**8**:593-611

[16] Galal A, Atta NF, Ali SM. Optimization of the synthesis conditions for $LaNiO_3$ catalyst by microwave assisted citrate method for hydrogen production. Applied Catalysis, A: General. 2011;**409-410**:202-208

[17] Giang HT, Duy HT, Ngan PQ, Thai GH, Thu DTA, Thu DT, et al. Hydrocarbon gas sensing of nano-crystalline perovskite oxides $LnFeO_3$ (Ln = La, Nd and Sm). Sensors and Actuators B: Chemical. 2011;**158**:246

[18] Ishihara T. In: Ishihara T, editor. Perovskite Oxide for Solid Oxide Fuel Cells, Fuel Cells and Hydrogen Energy. Springer Science Business Media, LLC; 2009. pp. 1-16 Chapter 1

[19] Atta NF, Galal A, El-Ads EH. Perovskite nanomaterials–Synthesis, characterization, and applications. In: Pan L, Zhu G, editors. Perovskite Materials–Synthesis, Characterisation, Properties, and Applications. Rijeka: IntechOpen, DOI: 10.5772/61280. Available from: https://www.intechopen.com/books/perovskite-materials-synthesis-characterisation-properties-and-applications/perovskite-nanomaterials-synthesis-characterization-and-applications

[20] Shao Z, Haile SM. A high-performance cathode for the next generation of solid-oxide fuel cells. Nature. 2004;**431**:170-173

[21] Shin J, Xu W, Zanella M, Dawson K, Savvin SN, Claridge JB, et al. Self-assembled dynamic perovskite composite cathodes for intermediate temperature solid oxide fuel cells. Nature Energy. 2017;**2**:16214

[22] Huang YH, Dass RI, Xing ZL, Goodenough JB. Double perovskites as anode materials for solid-oxide fuel cells. Science. 2006;**312**:254-257

[23] Song K, Lee K. Characterization of $Ba_{0.5}Sr_{0.5}M_{1-x}Fe_xO_{3-\delta}$ (M = Co and Cu) perovskite oxide cathode materials for intermediate temperature solid oxide fuel cells. Ceramics International. 2012;**38**:5123-5131

[24] Tongyun C, Liming S, Feng L, Weichang Z, Qianfeng Z, Xiangfeng C. $NdFeO_3$ as anode material for S/O_2 solid oxide fuel cells. Journal of Rare Earths. 2012;**30**(11):1138-1141

[25] Conceição LD, Silva AM, Ribeiro NFP, Souza MMVM. Combustion synthesis of $La_{0.7}Sr_{0.3}Co_{0.5}Fe_{0.5}O_3$ (LSCF) porous materials for application as cathode in IT-SOFC. Materials Research Bulletin. 2011;**46**:308-314

[26] Wang F, Chen D, Shao Z. $Sm_{0.5}Sr_{0.5}CoO_{3-\delta}$-infiltrated cathodes for solid oxide fuel cells with improved oxygen reduction activity and stability. Journal of Power Sources. 2012;**216**:208-215

[27] Vernoux P, Guillodo M, Fouletier J, Hammou A. Alternative anode material for gradual methane reforming in solid oxide fuel cells. Solid State Ionics. 2000;**135**:425-431

[28] Tao SW, Irvine JTS. A redox-stable efficient anode for solid-oxide fuel cells. Nature Materials. 2003;**2**:320-323

[29] Deganello F, Liotta LF, Leonardi SG, Neri G. Electrochemical properties of Ce-doped $SrFeO_3$ perovskites-modified electrodes towards hydrogen peroxide oxidation. Electrochimica Acta. 2016;**190**:939-947

[30] Wang J. Electrochemical glucose biosensors. Chemical Reviews. 2008;**108**:814-825

[31] Wang Y, Xu Y, Luo L, Dinga Y, Liu X, Huang A. A novel sensitive nonenzymatic glucose sensor based on perovskite $LaNi_{0.5}Ti_{0.5}O_3$-modified carbon paste electrode. Sensors and Actuators B. 2010;**151**:65-70

[32] Wang Y, Xu Y, Luo L, Ding Y, Liu X. Preparation of perovskite-type composite oxide $LaNi_{0.5}Ti_{0.5}O_3$–$NiFe_2O_4$ and its application in glucose biosensor. Journal of Electroanalytical Chemistry. 2010;**642**:35-40

[33] Liotta LF, Puleo F, La Parola V, Leonardi SG, Donato N, Aloisio D, et al. $La_{0.6}Sr_{0.4}FeO_{3-\delta}$ and $La_{0.6}Sr_{0.4}Co_{0.2}Fe_{0.8}O_{3-\delta}$ perovskite materials for H_2O_2 and glucose electrochemical sensors. Electroanalysis. 2014;**27**:1-10

[34] El-Ads EH, Galal A, Atta NF. Electrochemistry of glucose at gold nanoparticles modified graphite/$SrPdO_3$ electrode—Towards a novel non-enzymatic glucose sensor. Journal

of Electroanalytical Chemistry. 2015;**749**:42-52

[35] Wolkoff P. Volatile organic compounds sources, measurements, emissions, and the impact on indoor air quality. Indoor Air. 1995;**5**:5

[36] Boor BE, Spilak MP, Laverge J, Novoselac A, Xu Y. Human exposure to indoor air pollutants in sleep microenvironments: A literature review. Building and Environment. 2017;**125**:528

[37] Joshi N, Hayasaka T, Liu Y, Liu H, Oliveira ON, Lin L. A review on chemiresistive room temperature gas sensors based on metal oxide nanostructures, graphene and 2D transition metal dichalcogenides. Microchimica Acta. 2018;**185**:213

[38] Zheng H, Ou JZ, Strano MS, Kaner RB, Mitchell A, Kalantarzadeh K. Nanostructured tungsten oxide—Properties, synthesis, and applications. Advanced Functional Materials. 2011;**21**:2175

[39] Bai J, Zhou B. Titanium dioxide nanomaterials for sensor applications. Chemical Reviews. 2014;**114**:10131

[40] Thirumalairajan S, Girija K, Mastelaro VR, Ponpandian N. Surface morphology-dependent room-temperature $LaFeO_3$ nanostructure thin films as selective NO_2 gas sensor prepared by radio frequency magnetron sputtering. ACS Applied Materials & Interfaces. 2014;**6**:13917-13927

[41] Jun-Chao D, Hua-Yao L, Ze-Xing C, Xiao-Dong Z, Guo X. $LaCoO_3$–based sensors with high sensitivity to carbon monoxide. RSC Advances. 2015;**5**:65668-65673

[42] Ghasdi M, Alamdari H, Royer S, Adnot A. Electrical and CO gas sensing properties of nanostructured $La_{1-x}Ce_xCoO_3$ perovskite prepared by activated reactive synthesis. Sensors and Actuators B. 2011;**156**:147-155

[43] Sowmya P, Kaushik SD, Siruguri V, Diptikanta S, Viegas AE, Chandrabhas N, et al. Investigation of Ca substitution on the gas sensing potential of $LaFeO_3$ nanoparticles towards low concentration SO_2 gas. Dalton Transactions. 2016;**45**(34):13547-13555

[44] Zhang R, Jifan H, Zhouxiang H, Ma Z, Zhanlei W, Yongjia Z, et al. Electrical and CO-sensing properties of $NdFe_{1-x}Co_xO_3$ perovskite system. Journal of Rare Earths. 2010;**28**(4):591-595

[45] Benali A, Azizi S, Bejar M, Dhahri E, Graça MFP. Structural, electrical and ethanol sensing properties of double-doping $LaFeO_3$ perovskite oxides. Ceramics International. 2014;**40**(9):14367-14373

[46] Rong O, Zhang Y, Hu J, Li K, Wang H, Chen M, et al. Design of ultrasensitive Ag-$LaFeO_3$ methanol gas sensor based on quasi molecular imprinting technology. Scientific Reports. 2018;**8**:14220

[47] Yumin Z, Qingju L, Jin Z, Qin Z, Zhu Z. High sensitive and selective formaldehyde gas sensor using molecular imprinting technique based on Ag-$LaFeO_3$. Journal of Materials Chemistry C. 2014;**2**:10067

[48] Wang Y, Chen J, Wu X. Preparation and gas-sensing properties of perovskite-type $SrFeO_3$ oxide. Materials Letters. 2001;**49**:361-364

[49] Carotta MC, Butturi MA, Martinelli G, Sadaoka Y, Nunziante P, Traversa E. Microstructural evolution of nanosized $LaFeO_3$ powders from the thermal decomposition of a cyano-complex for thick film gas sensors. Sensors and Actuators B. 1997;**44**:590-594

[50] Sen S, Chakraborty N, Rana P, Narjinary M, Mursalin SD, Tripathy S, et al. Nanocrystalline gallium ferrite: A novel material for sensing very low concentration of alcohol vapour. Ceramics International. 2015;**41**:10110

[51] Sahner K, Moos R, Matam M, Tunney JJ, Post M. Hydrocarbon sensing with thick and thin film p-type conducting perovskite materials. Sensors and Actuators B. 2005;**108**:102-112

[52] Zhang D et al. Microwave-assisted synthesis of porous and hollow α-Fe_2O_3/$LaFeO_3$ nanostructures for acetone gas sensing as well as photocatalytic degradation of methylene blue. Nanotechnology. 2020;**31**:215601

[53] Francesco B, Ada F, Valerio V, Marco M, Rossella B. Optimization of perovskite gas sensor performance: Characterization, measurement and experimental design. Sensors. 2017;**17**:1352

[54] Yaoyu Y, Yanbai S, Pengfei Z, Rui L, Ang L, Sikai Z, et al. Fabrication, characterization and n-propanol sensing properties of perovskite-type $ZnSnO_3$ nanospheres based gas sensor. Applied Surface Science. 2020;**509**:145335

[55] Neeru S, Himmat KS, Sharma SK, Sachdev K. Fabrication of $LaFeO_3$ and rGO-$LaFeO_3$ microspheres based gas sensors for detection of NO_2 and CO. RSC Advances. 2020;**10**:1297-1308

[56] Wang H, Guo Z, Wentao H, Li S, Yongjia Z, Ensi C. Ethanol sensing characteristics of $BaTiO_3$/$LaFeO_3$ nanocomposite. Materials Letters. 2019;**234**:40-44

[57] Dong G, Huiqing F, Hailin T, Jiawen F, Qiang L. Gas-sensing and electrical properties of perovskite structure p-type barium-substituted bismuth ferrite. RSC Advances. 2015;**5**:29618-29623

[58] Silu P, Min M, Weijie Y, Ziqian W, Zihan W, Jian B, et al. Acetone sensing with parts-per-billion limit of detection using a $BiFeO_3$-based solid solution sensor at the morphotropic phase boundary. Sensors and Actuators B: Chemical. 2020;**313**:128060

[59] Tie Y, Ma SY, Pei ST, Zhang QX, Zhu KM, Zhang R, et al. Pr doped $BiFeO_3$ hollow nanofibers via electrospinning method as a formaldehyde sensor. Sensors and Actuators B: Chemical. 2020;**308**:127689

[60] Jain GH, Patil LA, Wagh MS, Patil DR, Patil SA, Amalnerkar DP. Surface modified $BaTiO_3$ thick film resistors as H_2S gas sensors. Sensors and Actuators B. 2006;**117**:159-165

[61] Patil RP, Gaikwad SS, Karanjekar AN, Khanna PK, Jain GH, Gaikwad VB, et al. Optimization of strontium- doping concentration in $BaTiO_3$ nanostructures for room temperature NH_3 and NO_2 gas sensing. Materials Today Chemistry. 2020;**16**:100240

[62] Artem M, Marina R, Alexander B, Alexander G. Nanocrystalline $BaSnO_3$ as an alternative gas sensor material: Surface reactivity and high sensitivity to SO_2. Materials. 2015;**8**:6437-6454

[63] Gopal Reddy CV, Manorama SV, Rao VJ. Preparation and characterization of barium stannate: Application as a liquefied petroleum gas sensor. Journal of Materials Science: Materials in Electronics. 2001;**12**:137-142

[64] Katekani S, Swart HC, Mhlongo GH. $LaBO_3$ (B = Fe, Co) nanofibers and their structural, luminescence and gas sensing characteristics. Physica B: Physics of Condensed Matter. 2020;**578**:411883

[65] Shaikh JS, Shaikh NS, Sheikh AD, Mali SS, Kale AJ, Kanjanaboos P, et al.

Perovskite solar cells: In pursuit of efficiency and stability. Materials and Design. 2017;**136**:54

[66] Newcomer juices up the race to harness sunlight. Science. 2013;**342**:1438-1439. DOI: 10.1126/science.342.6165.1438-b

[67] Gholipour S, Saliba M. From exceptional properties to stability challenges of perovskite solar cells. Small. 2018;**14**:1802385

[68] Kojima A, Teshima K, Shirai Y, Miyasaka T. Organometal halide perovskite as visible-light sensitizer for photovoltaic cells. Journal of the American Chemical Society. 2009;**131**:6050-6051

[69] Yang WS, Noh JH, Jeon NJ, Kim YC, Ryu S, Seo J, et al. High-performance photovoltaic perovskite layers fabricated through intramolecular exchange. Science. 2015;**348**:1234-1237

[70] Yin WJ, Yang JH, Kang J, Yan Y, Wie SH. Halide perovskite materials for solar cells: A theoretical review. Journal of Materials Chemistry. 2015;**3**:8926-8942

[71] Green MA, Baillie AH, Snaith HJ. The emergence of perovskite solar cells. Nature Photonics. 2014;**8**:506-514

[72] Babayigit A, Ethirajan A, Muller M, Conings B. Toxicity of organometal halide perovskite solar cells. Nature Materials. 2016;**15**:247-251

[73] Flora G, Gupta D, Tiwari A. Toxicity of lead: A review with recent updates. Interdisciplinary Toxicology. 2012;**5**:47-58

[74] Benmessaoud IR, Mahul-Mellier A-L, Horv'ath E, Maco B, Spina M, Lashuel HA, et al. Health hazards of methylammonium lead iodide based perovskites: Cytotoxicity studies. Toxicological Research. 2016;**5**:407-419

[75] Gong J, Darling SB, You F. Perovskite photovoltaics: Lifecycle assessment of energy and environmental impacts. Energy & Environmental Science. 2015;**8**:1953-1968

[76] Fthenakis VM, Kim HC, Alsema E. Emissions from photovoltaic life cycles. Environmental Science & Technology. 2008;**42**:2168-2174

[77] Antonio A. Perovskite solar cells go lead free. Joule. 2017;**1**:659-664

[78] Hoefler SF, Trimmel G, Rath T. Progress on lead-free metal halide perovskite for photovoltaic applications: A review. Monatshefte fuer Chemie. 2017;**148**:795-826

[79] Noel NK, Stranks SD, Abate A, Wehrenfennig C, Guarnera S, Haghighirad AB, et al. Lead-free organic-inorganic tin halide perovskites for photovoltaic applications. Energy & Environmental Science. 2014;**7**:3061-3068

[80] Hao F, Stoumpos CC, Cao DH, Chang RP, Kanatzidis H. Lead-free solid-state organic-inorganic halide perovskite solar cells. Nature Photonics. 2014;**8**(8):489-494

[81] Mandapu U, Vedanayakam SV, Thyagarajan K, Reddy MR, Babu BJ. Design and simulation of high efficiency tin halide perovskite solar cells. International Journal of Renewable Energy Research. 2017;**7**:1603-1612

[82] Ngoc TV, Doan HT. Lead-free hybrid organic-inorganic perovskites or solar cell applications. Journal of Chemical Physics. 2020;**152**:014104

[83] Gagandeep, Mukhtiyar S, Ramesh K, Vinamrita S. Graphene as charge transport layers in lead free perovskite solar cell. Materials Research Express. 2019;**6**:115611

[84] Giorgi G, Yamashita K. Alternative, lead-free, hybrid organic-inorganic perovskites for solar applications: A DFT analysis. Chemistry Letters. 2015;**44**:826-828

[85] Krishnamoorthy T, Ding H, Yan C, Leong WL, Baikie T, Zhang Z, et al. Lead-free germanium iodide perovskite materials for photovoltaic applications. Journal of Materials Chemistry A. 2015;**3**:23829-23832

[86] Yang B, Chen J, Hong F, Mao X, Zheng K, Yang S, et al. Lead-free, air-stable all-inorganic cesium bismuth halide perovskite nanocrystals. Angewandte Chemie International Edition. 2017;**56**:12471-12475

[87] Lou Y, Fang M, Chen J, Zhao Y. Formation of highly luminescent cesium bismuth halide perovskite quantum dots tuned by anion exchange. Chemical Communications. 2018;**54**:3779-3782

[88] Nelson RD, Santra K, Wang Y, Hadi A, Petrich JW, Panthani MG. Synthesis and optical properties of ordered-vacancy perovskite cesium bismuth halide nanocrystals. Chemical Communications. 2018;**54**: 3640-3643

[89] Zuo C, Ding L. Lead-free perovskite materials $(NH_4)_3Sb_2I_xBr_{9-x}$. Angewandte Chemie International Edition. 2017;**56**:6528-6532

[90] Saparov B, Hong F, Sun J-P, Duan H-S, Meng W, Cameron S, et al. Thin-film preparation and characterization of $Cs_3Sb_2I_9$: A lead-free layered perovskite semiconductor. Chemistry of Materials. 2015;**27**:5622-5632

[91] Hebig J-C, Kühn I, Flohre J, Kirchartz T. Optoelectronic properties of $(CH_3NH_3)_3Sb_2I_9$ thin films for photovoltaic applications. ACS Energy Letters. 2016;**1**:309-314

[92] Chen M, Ju M-G, Carl AD, Zong Y, Grimm RL, Gu J, et al. Cesium titanium(IV) bromide thin films based stable lead-free perovskite solar cells. Joule. 2018;**2**:558-570

[93] Li X, Zhong X, Hu Y, Li B, Sheng Y, Zhang Y, et al. Organic–inorganic copper(II)-based material: A low-toxic, highly stable light absorber for photovoltaic application. Journal of Physical Chemistry Letters. 2017;**8**:1804-1809

[94] Yang P, Liu G, Liu B, Liu X, Lou Y, Chen J, et al. All-inorganic Cs_2CuX_4 (X = Cl, Br, and Br/I) perovskite quantum dots with blue-green luminescence. Chemical Communications. 2018;**54**:11638-11641

[95] Tze-Bin S, Takamichi Y, Shinji A, Kanatzidis Mercouri G. Performance enhancement of lead-free tin-based perovskite solar cells with reducing atmosphere-assisted dispersible additive. ACS Energy Letters. 2017;**2**(4):897-903

[96] Nishimura K, Kamarudin MA, Hirotani D, Hamada K, Shen Q, Iikubo S, et al. Lead-free tin-halide perovskite solar cells with 13% efficiency. Nano Energy. 2020;**74**:104858

[97] World Health Organization. Guidelines for Drinking Water Quality. 2nd ed. Geneva, Switzerland: Author; 1997

[98] Fu F, Wang Q. Removal of heavy metal ions from wastewaters: A review. Journal of Environmental Management. 2011;**92**:407-418

[99] Biswas AK, Tortajada C. Water quality management: An introductory frame work. Water Resources Management. 2011;**27**:5-11

[100] Taseidifar M, Makavipour F, Pashley RM, Rahman AM. Removal of heavy metal ions from water using ion flotation. Environmental Technology and Innovation. 2017;**8**:182-190

[101] Mohammed AA, Ebrahim SE, Alwared AI. Flotation and sorptive-flotation methods for removal of lead ions from wastewater using SDS as surfactant and barley husk as biosorbent. Journal of Chemistry. 2013:1-6

[102] Rauf MA, Qadri SM, Ashraf S, Al-Mansoori KM. Sorption and desorption of Pb^{2+} ions by dead *Sargassum* sp. biomass. Chemical Engineering Journal. 2009;**150**:90-95

[103] Zhanga D, Chun-li Z, Zhou P. Preparation of porous nano-calcium titanate microspheres and its adsorption behavior for heavy metal ion in water. Journal of Hazardous Materials. 2011;**186**:971-977

[104] Haron W, Sirimahachai U, Wisitsoraat A, Wongnawa S. Removal of Cd^{2+} and Pb^{2+} from water by $LaGdO_3$ perovskite. SNRU Journal of Science and Technology. 2017;**9**(3):544-551

[105] Zhang D, Wang M, Tan Y. Preparation of porous nano-barium-strontium titanate by sorghum straw template method and its adsorption capability for heavy metal ions. Acta Chimica Sinica: Chinese Edition. 2010;**68**(16):1641-1648

[106] Rao MP, Musthafa S, Wu JJ, Anandan S. Facile synthesis of perovskite $LaFeO_3$ ferroelectric nanostructures for heavy metal ion removal applications. Materials Chemistry and Physics. 2019;**232**:200-204

[107] Zhang X, Li H, Li Y, Shen W. Structural properties and catalytic activity of Sr-substituted $LaFeO_3$ perovskite. Chinese Journal of Catalysis. 2012;**33**:1109-1114

[108] Haron W, Wisitsoraat A, Sirimahachai U, Wongnawa S. Removal of toxic heavy metal ions from water with $LaAlO_3$ perovskite. Songklanakarin Journal of Science and Technology. 2018;**40**(5):993-1001

[109] Chen F, Yu C, Wei L, Fan Q, Ma F, Zeng J, et al. Fabrication and characterization of $ZnTiO_3$/$Zn_2Ti_3O_8$/ZnO ternary photocatalyst for synergetic removal of aqueous organic pollutants and Cr(VI) ions. Science of The Total Environment. 2020;**706**:136026

[110] Normala H, Soo YRG. Removal of heavy metals from textile wastewater using zeolite. Environment Asia. 2010;**3**:124-130

[111] CPCB (Central Pollution Control Board). Advance Methods for Treatment of Textile Industry Effluents. Publication No. RERES/7/2007. New Delhi: Government of India; 2007. Available from: https://www.researchgate.net/publication/280572135_advance_methods_for_treatment_of_textile_industry_effluents

[112] Asad S, Amoozegar MA, Pourbabaee AA, Sarbolouki MN, Dastgheib SMM. Decolorization of textile azo dyes by newly isolated halophilic and halotolerant bacteria. Bioresource Technology. 2007;**98**:2082-2088

[113] Ananthanarayanan Y, Natchimuthu K, Sudipta T, Soundarapandian K, Ramasundaram T. Environment-friendly management of textile mill wastewater sludge using epigeic earthworms: Bioaccumulation of heavy metals and metallothionein production. Journal of Environmental Management. 2020;**254**:109813

[114] Toledano Garcia D, Ozer LY, Parrino F, Ahmed M, Brudecki GP, Hasan SW, et al. Photocatalytic ozonation under visible light for the remediation of water effluents and its integration with an electro-membrane bioreactor. Chemosphere. 2018;**209**:534-541

[115] Matei E, Covaliu CI, Predescu A, Berbecaru A, Tarcea C, Predescu C. Remediation of wastewater with ultraviolet irradiation using a novel titanium (IV) oxide photocatalyst. Analytical Letters. 2019;**52**:2180-2187

[116] Neagu S, Cojoc R, Enache M, Mocioiu OC, Precupas A, Popa VT, et al. Biotransformation of waste glycerol from biodiesel industry in carotenoids compounds by halophilic microorganisms. Waste and Biomass Valorization. 2019;**10**:45-52

[117] Kamińska G, Dudziak M, Kudlek E, Bohdziewicz J. Preparation, characterization and adsorption potential of grainy halloysite-CNT composites for anthracene removal from aqueous solution. Nanomaterials. 2019;**9**:890

[118] Wang J, Zhuang S. Removal of various pollutants from water and wastewater by modified chitosan adsorbents. Critical Reviews in Environmental Science and Technology. 2017;**47**:2331-2386

[119] Xu S, Zhang S, Chen K, Han J, Liu H, Wu K. Biosorption of La^{3+} and Ce^{3+} by *Agrobacterium* sp. HN1. Journal of Rare Earths. 2011;**29**:265-270

[120] Yagub MT, Sen TK, Afroze S, Ang HM. Dye and its removal from aqueous solution by adsorption: A review. Advances in Colloid and Interface Science. 2014;**209**:172-184

[121] Almasri DA, Saleh NB, Atieh MA, McKay G, Ahzi S. Adsorption of phosphate on iron oxide doped halloysite nanotubes. Scientific Reports. 2019;**9**:3232

[122] Ali SM, Eskandrani AA. The sorption performance of cetyl trimethyl ammonium bromide-capped $La_{0.9}Sr_{0.1}FeO_3$ perovskite for organic pollutants from industrial processes. Molecules. 2020;**25**(7):1640

[123] Chu Y, Tan X, Shen Z, Liu P, Han N, Kang J, et al. Efficient removal of organic and bacterial pollutants by Ag-$La_{0.8}Ca_{0.2}Fe_{0.94}O_{3-\delta}$ perovskite via catalytic peroxymonosulfate activation. Journal of Hazardous Materials. 2018;**356**:53-60

[124] Pratibha S, Dhananjaya N, Manjunatha CR, Narayana A. Fast adsorptive removal of direct blue-53 dye on rare-earth doped Lanthanum aluminate nanoparticles: Equilibrium and kinetic studies. Materials Research Express. 2019;**6**:1250i5

[125] Dong Z, Ye T, Zhao Y, Yu J, Wang F, et al. Perovskite $BaZrO_3$ hollow micro- and nanospheres: Controllable fabrication, photoluminescence and adsorption of reactive dyes. Journal of Materials Chemistry. 2011;**21**:5978

[126] Siddharth S, Soumitra M, Sonia R, Hari R, Bisht RS, Panigrahi SK, et al. Ti doped $BaMnO_3$ perovskite structure as photocatalytic agent for the degradation of noxious air and water pollutants. SN Applied Sciences. 2020;**2**:310